

Fig. S1. *Cog7* does not accumulate at the cleavage site of telophase spermatocytes. Selected frames (Phase contrast and corresponding fluorescence images) of a time lapse from a spermatocyte expressing GFP-*Cog7* undergoing telophase. GFP does not accumulate at the cleavage furrows (CF). Bar, 10 μ m.

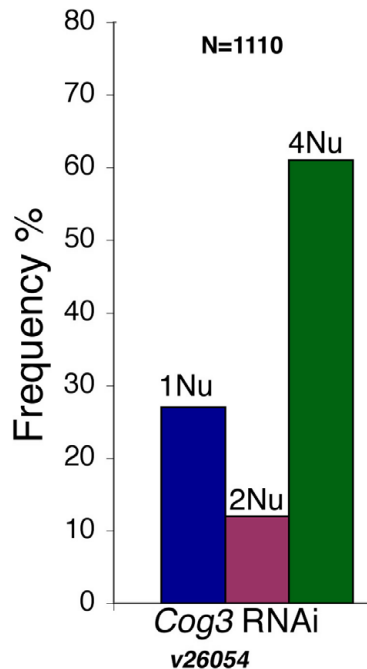


Fig. S2. Frequencies of spermatids containing 1, 2, or 4 nuclei per each NK in testes from males expressing dsRNA against *CG3248*, the *Drosophila Cog3* (*Cog3*). *UAS::DCog3-RNAi* was expressed in male meiosis using Bam-GAL4 (Chen and McKearin, 2003). The frequency of multinucleate spermatids in the Bam-GAL4 stock (used as a control) was zero.

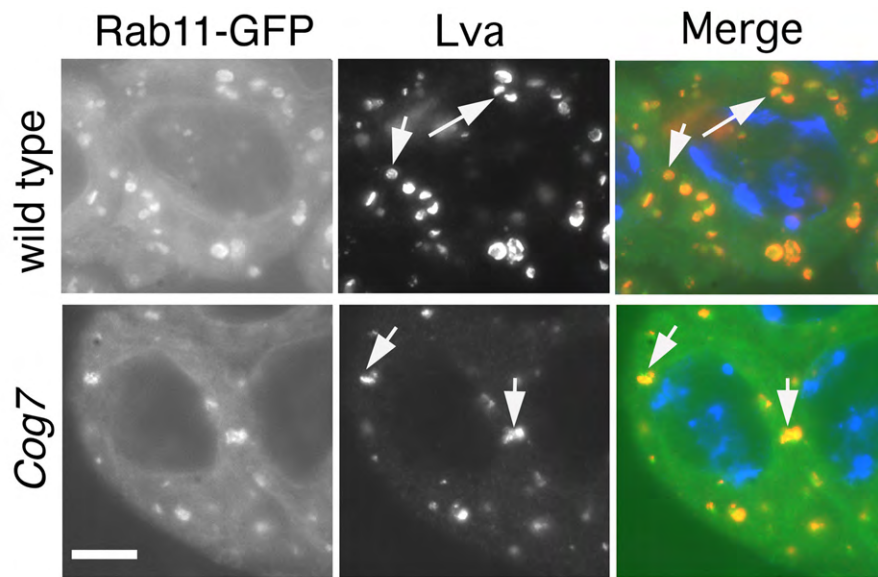


Fig. S3. Localisation of Rab11-GFP in prophase spermatocytes from wild type and *Cog7* males. Prophase spermatocytes expressing Rab11-GFP (green) were fixed and stained for Lva (red) and DNA (blue). Arrows point to Golgi stacks. Bar, 10 μ m

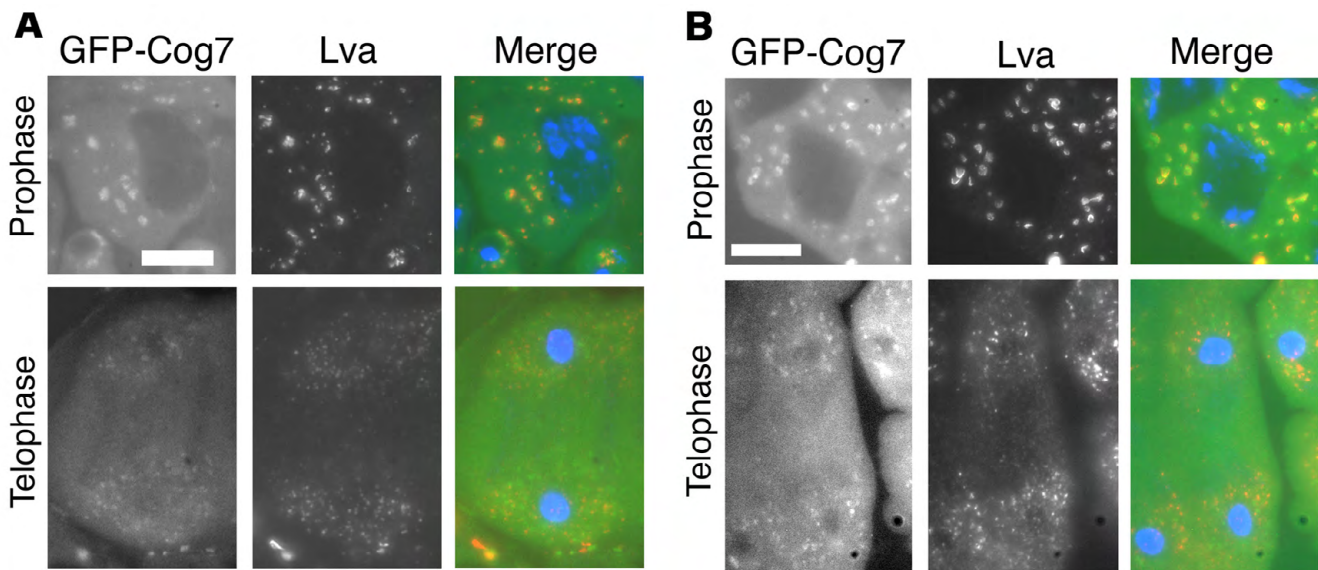


Fig. S4. Localisation of GFP-Cog7 in spermatocytes from *gio* and *Rab11* is comparable to wild type. Spermatocytes expressing GFP-Cog7 (green) from GFP-Cog7; *gio*³⁹³⁴/*Df(3R)D1-BX12* (A) and GFP-Cog7; *Rab11*^{eTo11}/*Rab11*^{93Bi} (B) males were fixed and stained for Lva (red) and DNA (blue). Bar, 10 μ m

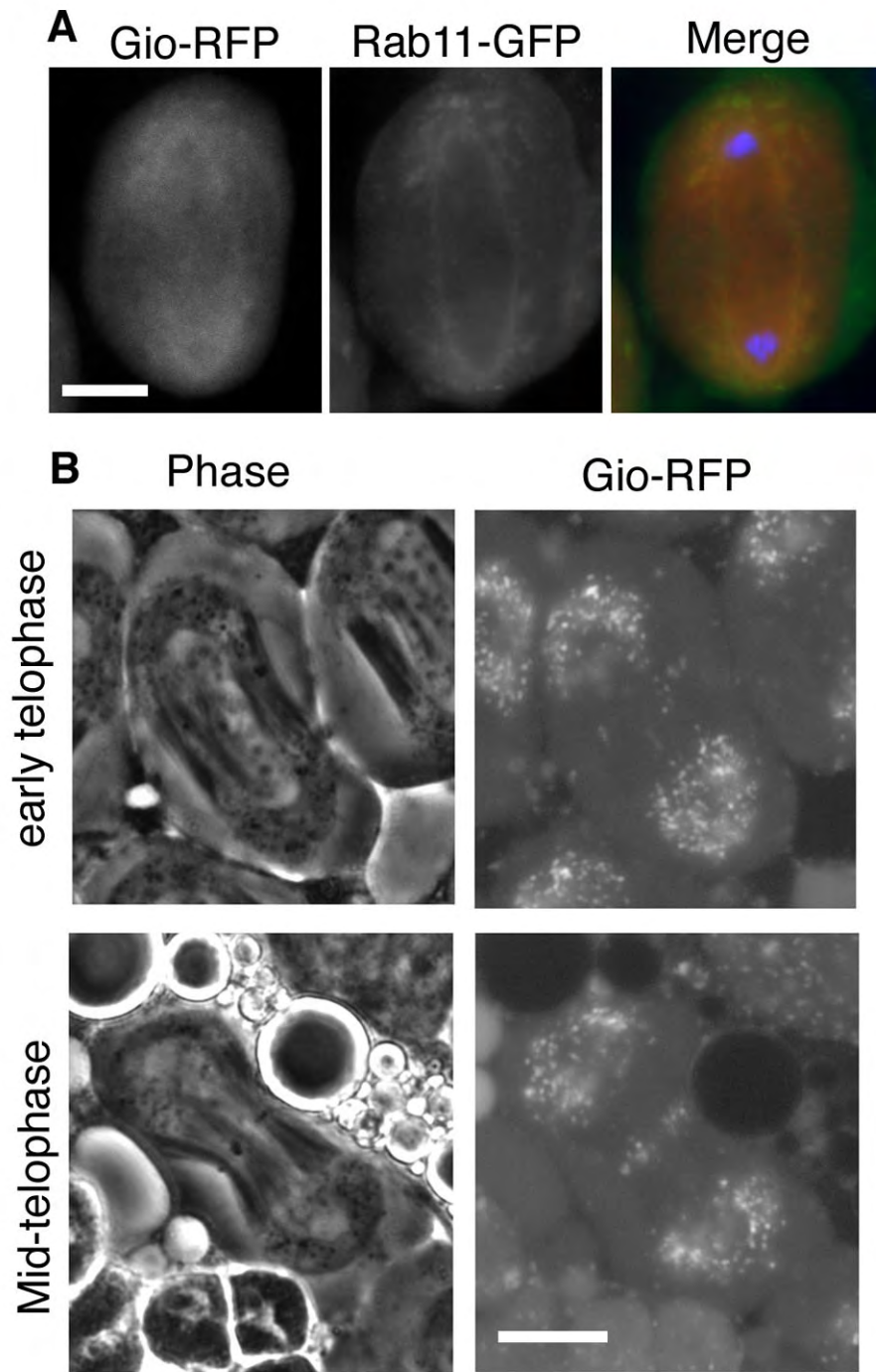


Fig. S5. Gio-RFP colocalizes with Rab11-GFP in dividing spermatocytes and concentrates at the cleavage furrow during telophase. (A) Spermatocyte expressing both Rab11-GFP (green) and Gio-RFP (red), were fixed and stained for DNA (blue). (B) Live dividing spermatocytes expressing Gio-RFP during early telophase and mid-telophase. Panels show phase contrast images (Phase) and corresponding fluorescence images. Bar, 10 μ m

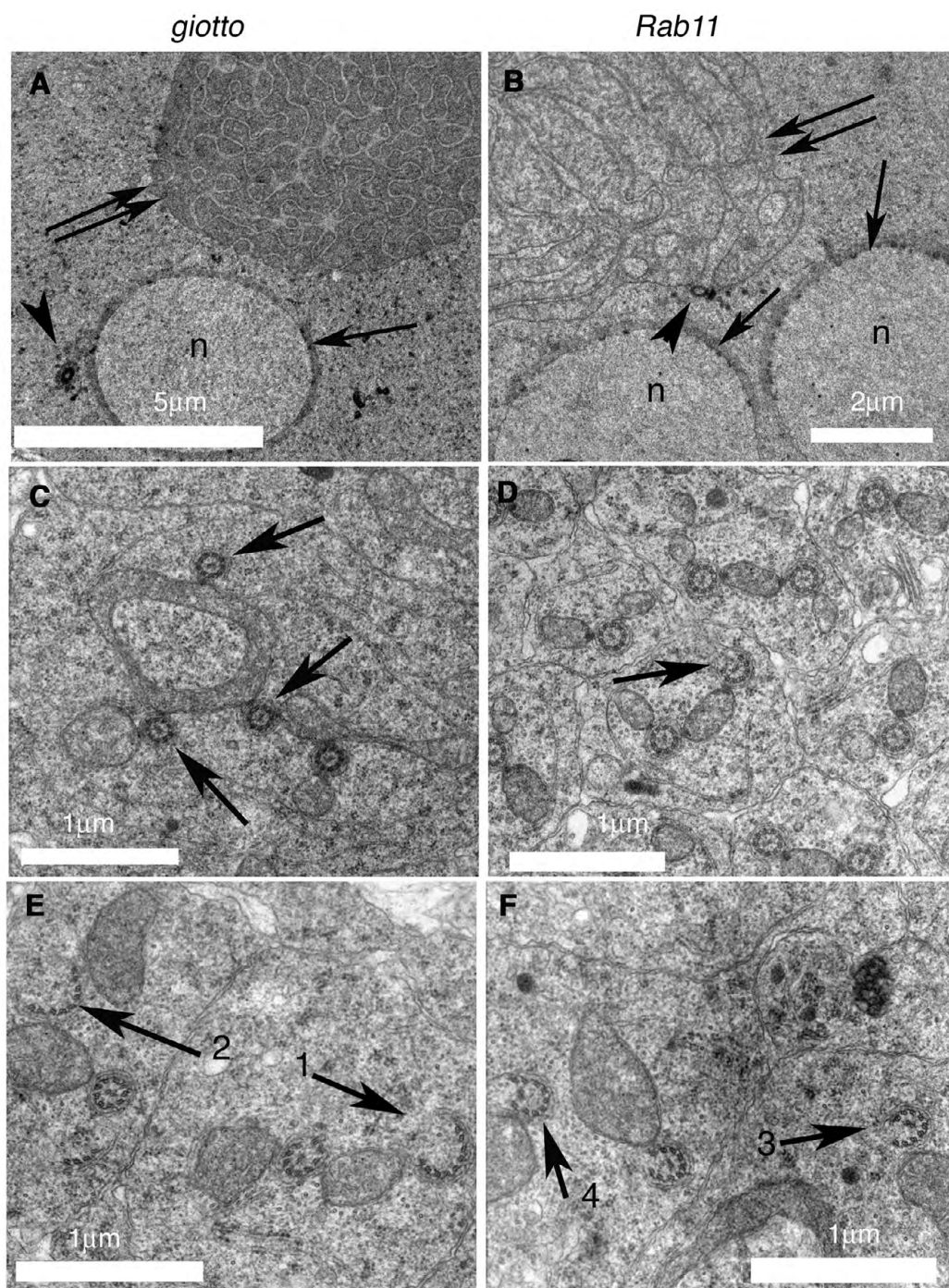


Fig. S6. Spermatids from *gio* and *Rab11* males display defects in basal body docking and axonemal structure. (A,B) TEM micrographs from *gio*³⁹³⁴/*Df(3R)D1-BX12* (A) and *Rab11*^{e(To)11}/*Rab11*^{93Bi} (B) spermatids. Arrowheads in A and B point to basal bodies. Nuclei (n), nuclear envelopes (arrow) and mitochondrial derivatives (double arrows) are indicated. (C-F) TEM micrographs showing axonemes in *gio*³⁹³⁴/*Df(3R)D1-BX12* (C,E) and *Rab11*^{e(To)11}/*Rab11*^{93Bi} (D,F) mutant spermatids. (C) Arrows point to three regular axonemes associated with a large mitochondrial derivative. (D) Arrow points to an irregular axoneme that lacks two peripheral doublets. (E,F) One axoneme in E lacks internal central microtubules (1, arrow). Other axonemes exhibit an irregular splayed structure (2, 3, 4 arrows).

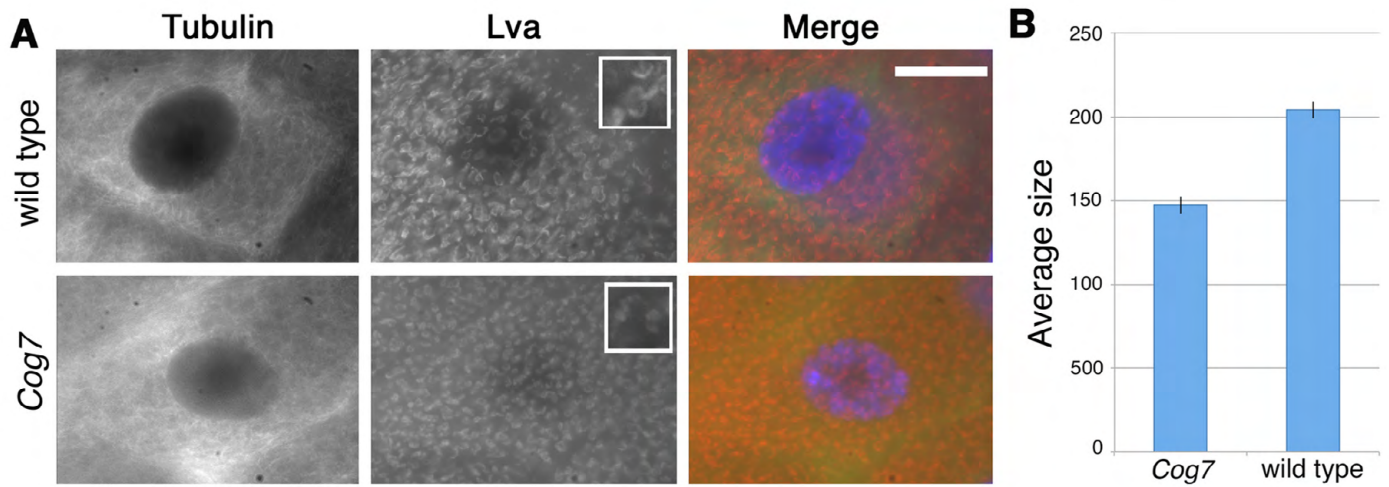


Fig. S7. Loss of *Cog7* affects the size of Golgi in larval salivary gland cells. (A) Salivary glands were stained for Lva (red), tubulin (green) and DNA (blue). Insets show higher magnifications. (B) Average area of Golgi bodies (\pm SEM) expressed in arbitrary units.